

University of Groningen

## Detection of grain-boundary resistance to slip transfer using nanoindentation

Soer, WA; De Hosson, J.T.M.

*Published in:*  
Materials Letters

*DOI:*  
[10.1016/j.matlet.2005.03.075](https://doi.org/10.1016/j.matlet.2005.03.075)

**IMPORTANT NOTE: You are advised to consult the publisher's version (publisher's PDF) if you wish to cite from it. Please check the document version below.**

*Document Version*  
Publisher's PDF, also known as Version of record

*Publication date:*  
2005

[Link to publication in University of Groningen/UMCG research database](#)

*Citation for published version (APA):*

Soer, W. A., & De Hosson, J. T. M. (2005). Detection of grain-boundary resistance to slip transfer using nanoindentation. *Materials Letters*, 59(24-25), 3192-3195. DOI: 10.1016/j.matlet.2005.03.075

**Copyright**

Other than for strictly personal use, it is not permitted to download or to forward/distribute the text or part of it without the consent of the author(s) and/or copyright holder(s), unless the work is under an open content license (like Creative Commons).

**Take-down policy**

If you believe that this document breaches copyright please contact us providing details, and we will remove access to the work immediately and investigate your claim.

*Downloaded from the University of Groningen/UMCG research database (Pure): <http://www.rug.nl/research/portal>. For technical reasons the number of authors shown on this cover page is limited to 10 maximum.*

# Detection of grain-boundary resistance to slip transfer using nanoindentation

W.A. Soer, J.Th.M. De Hosson\*

*Department of Applied Physics, Materials Science Center and Netherlands Institute for Metals Research,  
University of Groningen, Nijenborgh 4, 9747 AG Groningen, The Netherlands*

Received 1 January 2005; accepted 31 March 2005  
Available online 13 June 2005

## Abstract

Nanoindentation measurements near a high-angle grain boundary in a Fe-14%Si bicrystal showed dislocation pile-up and transmission across the boundary. The latter is observed as a characteristic displacement jump, from which the Hall–Petch slope can be calculated as a measure for the slip transmission properties of the boundary.

© 2005 Elsevier B.V. All rights reserved.

*Keywords:* Nanoindentation; Grain boundaries; Yield phenomena; Iron alloys

## 1. Introduction

The properties of grain boundaries in metals have been subject to extensive research for decades due to their importance for macroscopic mechanical behavior. The hardening effect of boundaries in single-phase polycrystalline materials is commonly described by the proportionality factor  $k_y$  in the Hall–Petch relation

$$\sigma_y = \sigma_0 + k_y d^{-1/2} \quad (1)$$

where  $\sigma_y$  refers to the yield stress,  $d$  to the grain size and  $\sigma_0$  to the frictional stress. The classical Hall–Petch relationship is traditionally described in terms of a dislocation pile-up model causing stresses to activate dislocation sources in the neighboring grains or grain boundaries are regarded as dislocation barriers limiting the mean free path of the dislocations, thereby increasing strain hardening. For a review reference is made to [1]. The slope  $k_y$  is considered as the ability of the grain boundaries to resist transmission of slip and is typically determined from deformation tests on

specimens with varying grain sizes, giving an average value of  $k_y$  for all grain boundaries.

In particular systems, other obstacles may also bound dislocation activity and thus govern the pile-up distance. The yield stress of these systems has been observed to obey a similar  $d^{-1/2}$  dependence, where  $d$  is the characteristic distance between the obstacles. For example, Anand and Gurland [2] found that both cementite particles and (sub)grain boundaries affect the strengthening of spheroidized steel in a Hall–Petch type manner.

Subgranular microhardness testing has been used for a long time to measure grain boundary hardening due to solute segregation [3], i.e. solid-solution hardening. Some researchers (e.g. Lee et al. [4]) have attributed similar hardening observations near grain boundaries to the difficulty in transmission of slip across a boundary. In these and other experiments in literature, Ngan and Chiu [5] found a Hall–Petch type dependence of the hardness on the distance to the grain boundary, from which they calculated the Hall–Petch slope  $k_y$  as a measure of the resistance to slip transfer across the particular boundary. This approach is however much disputed, as further indentation measurements on grain boundaries in Ni<sub>3</sub>Al showed no appreciable hardening [6]. Recently, Soifer et al. [7] carried out ultra-low load (90  $\mu$ N) nanoindentation experiments on high-

\* Corresponding author.

*E-mail address:* [j.t.m.de.hosson@rug.nl](mailto:j.t.m.de.hosson@rug.nl) (J.Th.M. De Hosson).

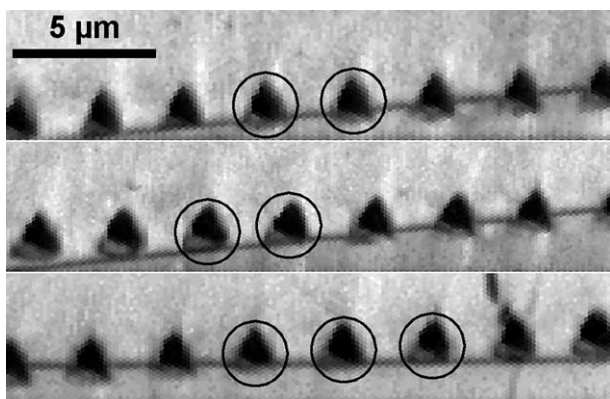


Fig. 1. EBSD scan of three lines of indents crossing the same grain boundary. The grayscale values indicate the quality of the Kikuchi pattern.

purity copper showing both hardening and softening effects within a few micrometers from the grain boundaries.

In this study, we present a new method for probing the slip transmission properties of an individual grain boundary using nanoindentation. The volume between the indenter and the boundary confines the dislocation pile-up in these experiments, leading to a dislocation burst across the boundary from which the Hall–Petch slope is calculated. The grain boundary resistance from slip transfer is thus determined independently of any hardening effect.

## 2. Experimental procedure

To accomplish an isolated and well-defined edge-on grain boundary, a Fe-14 wt.%Si alloy bicrystal was used. The surface was polished using a final polishing colloidal silica suspension. Electron backscatter diffraction (EBSD) was employed to locate the grain boundary with respect to a grid of marker indents. Additionally, the EBSD analysis provided the boundary misorientation, which is represented by a  $(-0.293, 0.120, 0.026)$  Rodrigues vector and does not correspond to any low-index coincident site lattice (CSL) boundary in body-centered cubic crystallography.

The nanoindentation measurements were carried out with a pyramidal Berkovich tip using the continuous stiffness measurement (CSM) technique [8]. In order to vary the distance to the grain boundary with the smallest possible increments, lines of indentations were drawn across the grain boundary at very low angles ( $<3^\circ$ ). The azimuthal orientation of the indenter was chosen to have one side of the triangular impression of the Berkovich tip parallel to the boundary. The maximum indentation depth was 200 nm; the spacing between indentations was 3  $\mu\text{m}$ . To exclude the possibility of mutual interaction between the plastically deformed zones of subsequent indentations, we compared lines of indents with spacings ranging from 3 to 10  $\mu\text{m}$  in the matrix of the bicrystal; no significant deviations in the

load-displacement data and the calculated hardness values were found.

## 3. Results and discussion

### 3.1. Observation of slip transmission

Results were obtained from three lines of 60 indents crossing the same grain boundary. Fig. 1 shows EBSD scans of the boundary crossings. For the circled indentations, a typical displacement jump is observed during the loading part of the indentation (Fig. 2). None of the indents in the matrix show this behavior.

The jump is attributed to a dislocation burst following pile-up at the grain boundary. The bursts are only observed when one side of the indenter is facing the boundary. This was verified by an additional measurement with the indenter rotated  $180^\circ$  to eliminate the possibility that this observation is due to the crystallographic asymmetry across the boundary. The orientation dependence can be understood by approximating the stress field by a uniaxial pressure component perpendicular to the faces of the indenter, and recognizing that the resolved shear stress at the grain boundary is a maximum when one side is facing the boundary.

From Fig. 1 it is apparent that some of the circled indents cross over the boundary at the maximum indentation depth; however, from the load-displacement data and the indenter geometry it is readily concluded that the indenter is still well away from the boundary at the instant of the dislocation burst. The occurrence of the burst is strongly related to the distance between the indent and the grain boundary. If an indentation is made too far from the boundary, the pile-up shear stress at the boundary will not reach the critical stress value needed for slip transfer. On the other hand, if the indent is too close, the indenter will cross over the boundary before this value is reached, and no dislocation burst will

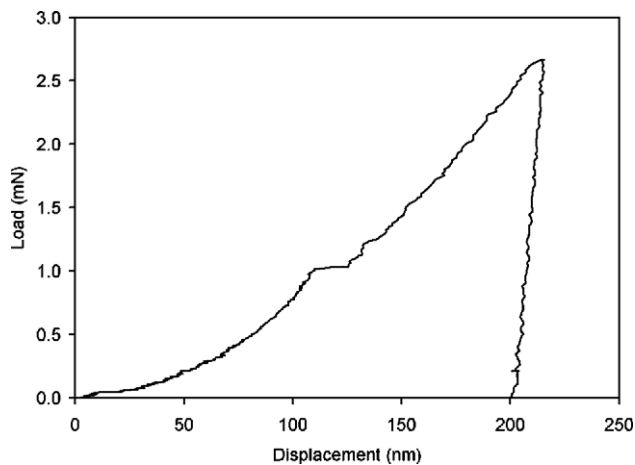


Fig. 2. Load-displacement curve of one of the circled indentations in Fig. 1, showing a typical displacement jump during loading.

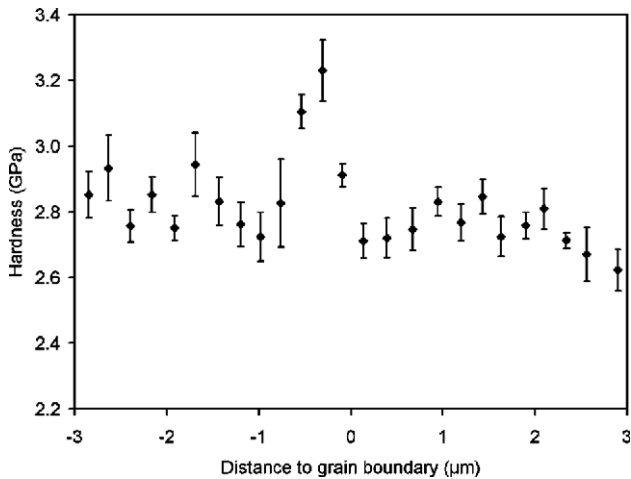


Fig. 3. CSM hardness as a function of the distance from the center of the indent to the grain boundary. Significant hardening is observed only in the grain where one side of the indenter is facing the boundary (i.e. where the distance is negative). Each data point represents the statistical average of five measurements.

occur. Therefore, only very few indentations show the displacement jump; their distance to the boundary (measured from the center of the indent) ranges from 0.3 to 0.7  $\mu\text{m}$ .

Prior to slip transmission across the boundary, the accumulated stress appears as an increase in the measured CSM hardness. After the burst, the hardness is comparable to the values measured away from the boundary. Therefore, a peak is observed in the average hardness as a function of distance to the grain boundary, as shown in Fig. 3. Significant hardening is measured only on the side of the boundary where the bursts occur; consequently, it is not ascribed to solute Si enrichment at the grain boundary [9]. The range over which the hardness increases is a few hundreds of nanometers, in contrast to a several micrometers in the measurements by Soifer et al. This could be due to the relative ease of cross slip in body-centered cubic materials, reducing the amount of pile-up at the boundary. The marginality of the hardening effect observed here suggests that reported measurements of grain boundary properties solely based on hardening should be viewed with caution.

### 3.2. Activated slip systems

Since the value of the Hall–Petch slope depends on the grain boundary parameters [10], the geometry of our

Table 1  
Favored slip systems in the pile-up grain

Slip system	Schmid factor	$\theta$ ( $^\circ$ )
(1 $\bar{1}$ 2) [ $\bar{1}$ 11]	0.489	16.4
(11 $\bar{2}$ ) [111]	0.488	84.8
( $\bar{1}$ 01) [111]	0.450	84.8
(101) [ $\bar{1}$ 11]	0.450	16.4
(112) [ $\bar{1}$ 1 $\bar{1}$ ]	0.434	71.6

experiment needs to be known in order for a complete analysis to be conducted. Using the EBSD information, we can calculate the favored slip systems on both sides of the boundary, assuming Schmid behavior as a first approximation. In the indented grain, we assume again a uniaxial compressive stress perpendicular to the faces of the Berkovich indenter and calculate the resolved shear stress for all possible slip systems on {110} and {112} planes. Table 1 shows the five most favored slip systems and their respective Schmid factors for an applied stress component along [0.004 -0.119 -0.993], which is the normal to the indenter face closest to the grain boundary. For each slip system, the angle  $\theta$  between the slip direction and the grain boundary normal vector [-0.752 0.558 0.352] is given as a measure for the pile-up distance. Accordingly, the highest pile-up shear stress is established on the (1 $\bar{1}$ 2) [ $\bar{1}$ 11] slip system, having the largest Schmid factor and the shortest pile-up distance.

To predict the activated slip systems in the adjacent grain, we use the geometric criterion proposed by Shen et al. [11]:

$$m = (\bar{L}_1 \cdot \bar{L}_2) * (\bar{g}_1 \cdot \bar{g}_2) \quad (2)$$

where  $L_1$  and  $L_2$  are the normalized intersection lines common to the slip planes and the boundary plane, and  $g_1$  and  $g_2$  are the normalized slip directions in the pile-up and emission grains. The factor  $m$  is a maximum for the favored slip system, i.e. the angle  $\alpha$  between the intersection lines and the angle  $\beta$  between the slip directions are to be minimized (see Fig. 4). The results of this optimization are summarized in Table 2. Assuming a dislocation pile-up in the indented grain on the (1 $\bar{1}$ 2) [ $\bar{1}$ 11] slip system as discussed above, we find that slip is transmitted easiest to the ( $\bar{1}$ 01) [111] system in the adjacent grain with  $m=0.82$ ,  $\alpha=16^\circ$  and  $\beta=32^\circ$ .

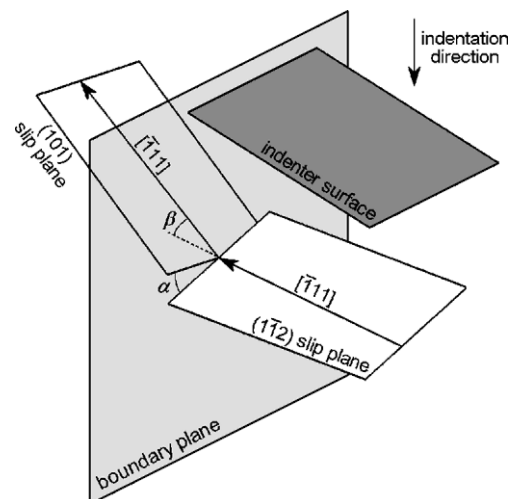


Fig. 4. Relative orientation of the slip systems, the grain boundary and the indenter.

Table 2  
Favored slip systems in the emission grain

Slip system	$m$	$\alpha$ (°)	$\beta$ (°)
(101) $[\bar{1}11]$	0.818	15.5	31.9
( $\bar{1}12$ ) $[1\bar{1}1]$	0.764	0.3	40.2
( $1\bar{1}2$ ) $[\bar{1}11]$	0.764	25.9	31.9
(011) $[1\bar{1}1]$	0.668	28.9	40.2
( $\bar{1}01$ ) $[1\bar{1}1]$	0.640	33.1	40.2

### 3.3. Hall–Petch slope calculation

The observed slip transfer occurs when the shear stress accumulated at the boundary is allowed to reach some critical value  $\tau^*$  before the indenter hits the adjacent grain. From the center positions of the indents and the recorded load-displacement data, we can calculate the distance  $d$  from the indenter to the boundary across the surface at the instant of slip transmission. Since dislocations are nucleated at the surface during indentation, this distance can be considered representative for the volume that bounds the dislocation pile-up. Measured values for  $d$  range from 0.11 to 0.34  $\mu\text{m}$ . With  $m$  representing the angles between the slip systems as in Eq. (2), the critical shear stress  $\tau^*$  is given by [13–16]

$$\tau^* = m(\tau_a - \tau_0) \sqrt{\frac{d}{4r}} \quad (3)$$

where  $\tau_a$  is the applied shear stress,  $\tau_0$  is the intrinsic frictional shear stress resisting dislocation motion inside the grain and  $r$  is the distance to the dislocation source in the adjacent grain. Setting  $k_y = 2m^{-1} \tau^* \sqrt{r}$  [16] gives the Hall–Petch type equation. Eq. (3) becomes

$$\tau_a = \tau_0 + \frac{k_y}{\sqrt{d}}. \quad (4)$$

Next, the applied shear stress  $\tau_a$  is estimated from the indentation load  $P$  and depth  $h$  for which the dislocation burst is observed. Using the contact area function  $A_c(h_c)$  of the indenter, and defining the contact depth  $h_c$  according to Oliver and Pharr [8], we find

$$\tau_a = \frac{\sigma}{2} = \frac{P}{2A_c(h_c)}. \quad (5)$$

Assuming  $\tau_0 = 200$  MPa [12], we calculate the average Hall–Petch slope to be  $k_y = 0.63$   $\text{MNm}^{-3/2}$  with a standard deviation of 0.09  $\text{MNm}^{-3/2}$ . Although literature values for the used Fe-14%Si alloy are not available, our result agrees well with the reported value for  $\alpha$ -Fe,  $k_y = 0.583$   $\text{MNm}^{-3/2}$  [17]. In order to verify the relation between  $k_y$  and the misorientation factor  $m$ , a systematic comparison of different grain boundaries using the presented approach would be interesting.

Typical  $k_y$  values for body-centered cubic metals at room temperature are on the order of 0.3–1.8  $\text{MNm}^{-3/2}$ . For most face-centered cubic metals, the Hall–Petch slope is an order of magnitude smaller (0.05–0.1  $\text{MNm}^{-3/2}$ ). For the

presented experimental method, this leads to a characteristic pile-up distance  $d$  that is two orders of magnitude smaller. Therefore, slip transmission is unlikely to be observed directly during indentation of these metals.

## 4. Conclusions

It was found that nanoindentation near a grain boundary leads to dislocation pile-up and subsequent propagation across the boundary. The latter is observed as a displacement jump in the loading curve of the indentation, from which a value for the Hall–Petch slope  $k_y$  can be derived using the fact that the dislocation pile-up is bounded by the indenter on one side and the grain boundary on the other side. The result agrees very well with literature values obtained from macroscopic deformation. No appreciable long-range grain boundary hardening was observed, making earlier reports of Hall–Petch slope calculations from such hardening disputable.

## Acknowledgements

The authors thank Pavel Lejcek of the Institute of Physics, Czech Republic for providing the Fe-Si bicrystal. This work was carried out under project number MC4.01104 within the framework of the Strategic Research Program of the Netherlands Institute for Metals Research.

## References

- [1] A. Lasalmonie, J.L. Strudel, J. Mater. Sci. 21 (1986) 1837.
- [2] L. Anand, J. Gurland, Metall. Trans., A, Phys. Metall. Mater. Sci. 7 (1976) 191.
- [3] K.T. Aust, R.E. Hanneman, P. Niessen, J.H. Westbrook, Acta Metall. 16 (1968) 291.
- [4] C.S. Lee, G.W. Han, R.E. Smallman, D. Feng, J.K.L. Lai, Acta Mater. 47 (1999) 1823.
- [5] A.H.W. Ngan, Y.L. Chiu, Mater. Res. Soc. Symp. Proc. 649 (2001) (Q4.10.1).
- [6] P.C. Wo, A.H.W. Ngan, J. Mater. Res. 19 (2004) 189.
- [7] Y.M. Soifer, A. Verdyan, M. Kazakevich, E. Rabkin, Scr. Mater. 47 (2002) 799.
- [8] W.C. Oliver, G.M. Pharr, J. Mater. Res. 7 (1992) 1564.
- [9] T. Watanabe, T. Murakami, S. Karashima, Scr. Metall. 12 (1978) 361.
- [10] J.W. Wyrzykowski, M.W. Grabski, Philos. Mag., A 53 (1986) 505.
- [11] Z. Shen, R.H. Wagoner, W.A.T. Clark, Acta Metall. 36 (1988) 3231.
- [12] R.W.K. Honeycombe, The Plastic Deformation of Metals, Edward Arnold, London, 1968.
- [13] N.J. Petch, J. Iron Steel Inst. 174 (1953) 25.
- [14] E.O. Hall, Proc. Phys. Soc. B64 (1951) 747.
- [15] J.P. Hirth, J. Lothe, Theory of Dislocations, McGraw Hill, New York, 1968.
- [16] T.H. Courtney, Mechanical Behavior of Materials, McGraw Hill, 1990, p. 169.
- [17] E. Anderson, D.L.W. King, Spreadborough, J. Trans. Metall. Soc. AIME 242 (1968) 115.